Strong magnetic surface anisotropy of ultrathin Fe on curved Pt(111)

Ruihua Cheng,[1] S. D. Bader,[2] and F. Y. Fradin[2]
[1]*Department of Physics, Indiana University–Purdue University–Indianapolis, 402 North Blackford Street, Indianapolis, Indiana 46202, USA*
[2]*Materials Science Division, Argonne National Laboratory, Argonne, Illinois 60439, USA*
(Received 19 June 2007; revised manuscript received 19 September 2007; published 3 January 2008)

We investigate the step decoration growth and magnetic properties of Fe grown on a curved Pt(111) single crystal by means of low-energy electron diffraction, scanning tunneling microscopy, and the surface magneto-optical Kerr effect. We find that the step-induced magnetic anisotropy enhances the Curie temperature of Fe ultrathin films. Fe grown on high-vicinal-angle surfaces has larger values of both the saturation magnetization M_s and coercivity H_c compared with the flat surface. $M_s(\alpha)$ increases quadratically with the vicinal angle α. The atomic steps of the vicinal surface greatly affect the magnetic properties of ultrathin Fe films. Finally we find that the step-induced surface anisotropy $K_s(\alpha)$ is proportional to α^4. The surface anisotropy of Fe on curved Pt(111) substrate is related to the numbers of atoms at the step edges and the polarization of proximal Pt atoms.

DOI: 10.1103/PhysRevB.77.024404 PACS number(s): 75.30.Gw, 75.70.Ak, 75.75.+a

INTRODUCTION

The study of low-dimensional magnetic epitaxial systems is of great interest due to their technical applications as well as their rich fundamental physics.[1] Compared with bulk structures, whose properties are well known, magnetic nanostructure are complex and manifest a wealth of variety. This is because the energies associated with various parameters are comparable in nanostructures. These parameters include the magnetocrystalline anisotropy,[2] shape anisotropy, surface anisotropy,[3] step anisotropy,[4] magnetoelastic effects,[5] and the interface between the material and substrate.[6] It is well known that an isolated one-dimensional (1D) chain with isotropic finite-range exchange interactions cannot maintain long-range ferromagnetic order at finite temperature.[7] Neither does the isotropic 2D Heisenberg system.[8] However, the presence of magnetic anisotropy, finite size, and nonequilibrium effects could break the symmetry and affect this conclusion.[8,9] Due to the unique structure of the stepped surface, it provides an ideal platform where different anisotropy terms come into prominence. Recently, a great deal of effort has been devoted to investigating 1D nanostripes[10–15] and 2D thin films[16,17] of magnetic transition metals on vicinal surfaces. The magnetic anisotropy is related to and affected by the local atomic and electronic structure. Understanding the nature of the magnetic anisotropy is crucial to the development of novel magnetic nanostructures. Both the magnetic moment and the magnetic anisotropy energy of 1D Co chains and 2D films are calculated to be enhanced with respect to bulk Co.[18–21] This enhancement is due to the symmetry breaking in the surface and the introduction of atomic steps on the vicinal substrate. To study the effect of step-induced anisotropy on magnetic properties, curved substrates are widely used to supply a continuous gradient in step density.[22] Different systems have been explored in this area. The magnetic anisotropy of Fe/Ag(001) (Refs. 23 and 24) and Fe/W(001) (Ref. 5) increases quadratically with step density. A quadratic dependence of anisotropy on step density can be explained based on Néel's pair bonding model,[25] and the consequence is that the anisotropy decays with film thickness d as $1/d$. The magnetic anisotropy of Fe/Pd(001) (Ref. 22) and Co/Cu(001) (Ref. 26) exhibits linear dependence on the step density. These works indicate that the result strongly depends on the material and substrate. To better understand the step-induced anisotropy, more research is needed to probe the different material-substrate systems.

In the present work we explore the magnetic properties of ultrathin Fe films grown on a curved Pt(111) substrate in the coverage range of 0–3.6 monolayers (ML). Pt is known to be nearly ferromagnetic and can have an induced magnetic moment when it is in proximity to 3d ferromagnetic atoms. The strong spin-orbit interaction in Pt produces a high value of the perpendicular magnetic anisotropy in the Fe/Pt system.[27] Both the saturated magnetization M_s and coercivity H_c of Fe grown on a high-vicinal-angle surface show larger values compared with the flat surface. We find that the step-induced magnetic anisotropy enhances the Curie temperature of ultrathin Fe films. The atomic steps of the vicinal surface greatly affect the magnetic properties of ultrathin Fe films. Finally, we find that the step-induced surface anisotropy $K_s(\alpha)$ depends on the vicinal angle α as $K_s(\alpha) \propto \alpha^4$. The surface anisotropy of Fe on a curved Pt(111) substrate is due to the step-induced magnetic anisotropy and the polarization of the proximal Pt atoms.

EXPERIMENTAL APPROACH

The experiments were carried out in an ultrahigh vacuum (UHV) chamber with base pressure below 5×10^{-11} Torr. The system is equipped with a scanning tunneling microscopy (STM), surface magneto-optical Kerr effect (SMOKE), Auger electron spectroscopy, low-energy electron diffraction (LEED), and reflective high-energy electron diffraction (RHEED) facilities. A Pt(111) single crystal with the size of 5×10 mm^3 was carefully polished into a cylindrical curved shape. It provides a continuous range of substrate from a flat Pt(111) surface ($\alpha=0$) up to vicinal angles of 15°, with an average terrace width down to 0.85 nm. The steps are along

the close-packed $[1\bar{1}0]$ direction and the vicinal angle α varying along the $[\bar{2}11]$ direction. The vicinal Pt(111) surface has straight atomic step arrays with a narrow terrace width distribution, which is attributed to repulsive interactions between adjacent steps.[28] The Pt crystal was loaded into our UHV chamber and cleaned *in situ* with repeated cycles of Ar sputtering at 900 eV followed by annealing at 1000 K. The substrate was also annealed in oxygen at 5×10^{-8} Torr for a few minutes to eliminate the surface carbon impurities. The resultant substrate is free of oxygen and carbon contamination within the Auger detection limit. Once the surface is atomically clean, Fe is deposited at room temperature with a low dose rate equivalent to 0.2 ML/min, as calibrated by RHEED and STM. During the deposition the chamber pressure was below 2×10^{-10} Torr. An Fe wedge was grown in the thickness range of 0–3.6 ML and it varies along the $[1\bar{1}0]$ direction. The film thickness and vicinal angle vary independently. Two hours after the Fe deposition SMOKE was used to study the magnetic properties along the wedge. The length of the wedge is 4 mm and the focused He-Ne laser beam size is 0.2 mm. Thus, the thickness gradient sampled for each data point corresponds to ±0.1 ML. We performed both longitudinal and polar geometry SMOKE studies for our samples in order to characterize the magnetic properties, while only polar data are presented in this paper.

RESULTS AND DISCUSSION

Both LEED and STM were used to check the quality of the substrate. An *in situ* STM image of the clean Pt(111) surface on the curved substrate with $\alpha=8°$ is shown in Fig. 1(a). At this vicinal angle the terrace width is about 1.6 nm. The STM image is displayed in the derivative mode (dz/dx) to highlight the step edges (where z is the height in a constant-tunneling-current scan mode, and x is measured in plane). The corresponding LEED pattern of the surface is shown in Fig. 1(b). The image shows elongated, split spots due to the change of step terrace width on the curved substrate. The average distance between the split spots yields a terrace width of ~seven atomic spacings which agrees with the STM data. As shown in Fig. 1(c), the split diffraction spots collapse into singlets as the vicinal angle is decreased to 0. There is no other sign of reconstruction and the background is negligible. The growth was studied by monitoring the RHEED intensity oscillations, as has been presented elsewhere.[29,30] According to the RHEED data, the initial growth of Fe is smooth layer-by-layer growth due to step decoration. Then the streaks start to blur and break into spots, indicating 3D growth. Thus, initially Fe grows pseudomorphically on the Pt substrate. Then the Fe lattice gradually starts to relax (real lattice spacing decreases) and the relaxation is observed after 1.6 ML. Due to the large lattice mismatch of 10.6% between Fe and Pt, complete relaxation occurs as Fe approaches a thickness of 4 ML. Large strain is built into the films below this thickness.

Both longitudinal and polar SMOKE measurements were made. For the longitudinal geometry the magnetic field was applied in plane along the step direction, while for the polar geometry the magnetic field was applied normal to the surface, which is perpendicular to the $[1\bar{1}0]$ step edge. The Kerr signal in remanence is proportional to the remanent magnetization M_r. We performed polar SMOKE measurements as a function of Fe thickness for different vicinal angles at room temperature. The data are shown in Figs. 2 and 3. Figure 2 illustrates the magnetic hysteresis loops measured at indi-

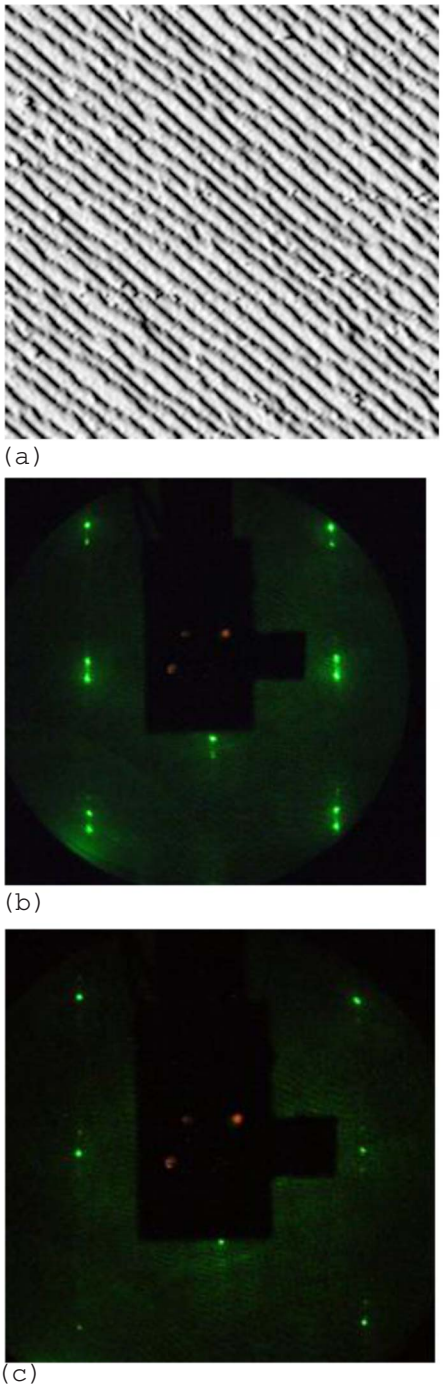

FIG. 1. (Color online) (a) STM images of the clean Pt(111) surface with vicinal angle of 8° and average terrace width ~1.6 nm. (The image size is 40×40 nm^2.) (b) the corresponding LEED pattern of the surface shown in (a). (c) LEED pattern of the flat Pt(111) surface.

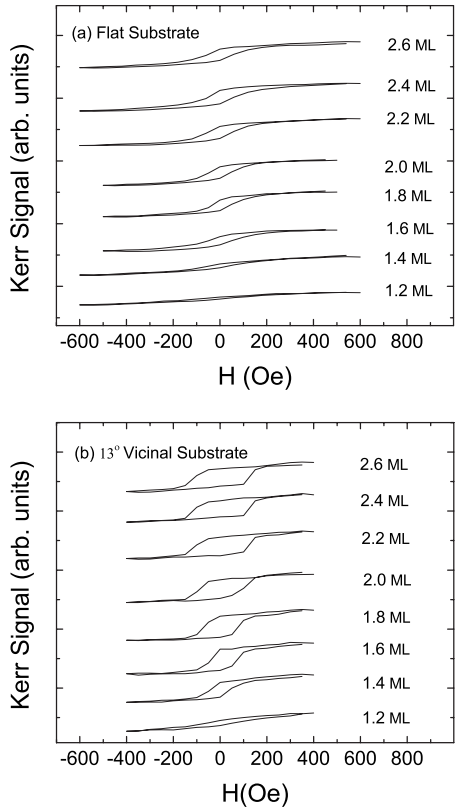

FIG. 2. Polar Kerr hysteresis loops at room temperature for Fe films grown on (a) flat Pt(111) surface and (b) stepped Pt(111) surface with vicinal angle of 13° with indicated Fe thickness. (The coordinate axis scale is the same for the two figures.)

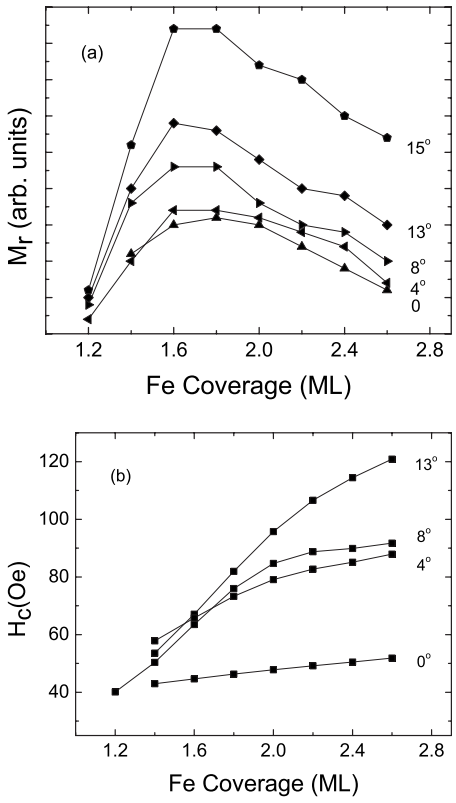

FIG. 3. Fe-coverage-dependent (a) remanent magnetization M_r and (b) coercivity H_c of Fe grown on curved Pt(111) substrate at the indicated vicinal angle measured at room temperature via polar Kerr effect.

cated Fe thickness deposited on the flat Pt(111) substrate (α=0) and a highly stepped surface with α=13°. (The linear background slope of the loops is from the UHV window or paramagnetic impurities in the substrate.) Notice that we use the same scales in these two figures. Comparing the data for α=0 and 13°, it is clear that the onset of long-range magnetic order requires a thicker Fe film (~1.5 ML) for α=0 than for α=13° (~1.2 ML). Since the Curie temperature T_c sensitively scales with the thickness of the ferromagnetic layer as 100–200 K/ML, the data indicate that the step surface enhances the Curie temperature. Variable-temperature measurements will be done in our laboratory to confirm the result. Theoretically it is known that the isotropic 2D Heisenberg model does not give rise to long-range magnetic order at finite temperature.[8] In our system, due to the symmetry breaking of the vicinal surface, the step-induced magnetic anisotropy results in the ferromagnetic order at finite temperature. In addition to the T_c enhancement, we also find that both M_s and H_c of Fe grown on a high-vicinal-angle surface have larger values compared to on the flat surface. The significant enhancement of Kerr signal is not likely completely caused by the Fe atoms, but from the additional induced moment of the proximal Pt atoms. It has been shown that Pt atoms in the interface with Fe atoms can have an induced magnetic moment due to the coupling with Fe via 3*d*-5*d* hybridization. As the step density increases with α, more Pt atoms are magnetically polarized by the Fe. For ultrathin Fe films, the contribution from Pt atoms plays an important role and the total M_s value of the system increases compared with the flat substrate. In the meantime on the vicinal surface the strong magnetic polarization of Pt substrate could also stabilize the long-range ferromagnetic order at a lower Fe thickness. As a result, it enhances the T_c value on the vicinal surface.

The magnetic reversal process is a combination of nucleation, expansion of domains through morphological constrictions, and the coherent rotation within domains. Compared with the flat surface, monatomic steps on the vicinal surface introduce more pinning sites and impede the motion of domain walls. As a result of that, the atomic steps cause an increase of the H_c value. In summation the magnetic properties of ultrathin Fe films is greatly altered by the step structure on a vicinal surface.

Figure 3 shows M_r and H_c measured at the indicated vicinal angles as a function of Fe thickness. We noticed that, above 3 ML coverage of Fe, only longitudinal hysteresis loops are observed, the polar signal being vanishingly small. The magnetic easy axis is in plane due to the shape anisotropy or demagnetization. As the Fe coverage decreases, the polar M_r first increases, as illustrated in Fig. 3(a), exhibiting full remanence at ~1.6 ML, and then decreases due to the decreased amount of Fe. We attribute the spin reorientation from in plane to perpendicular due to the competition between the shape anisotropy and the magnetocrystalline aniso-

tropy associated with the step edges.[31] Ultrathin Fe on stepped Pt(111) exhibits magnetic anisotropy perpendicular to the surface in our system. It appears to have a stronger surface anisotropy compared to Fe/Pd(110),[32] for which the spin reorientation occurs at 0.7 ML. One of the important sources of large magnetic anisotropy of the Fe-Pt system is the proximal polarization of the Pt atoms. Pt would contribute a stronger spin-orbit interaction than Pd due to its higher Z value.

Figure 3(b) shows the dependence of H_c as a function of the film thickness for different α values. The behavior is complex. Intuitively, we expect the coercive field to decrease with increasing film thickness, because the high anisotropy energy is dominated by the surface and step sites, and the ratio of the anisotropy energy to the total energy is proportional to the surface-to-volume ratio. However, this is not the case when the step-induced anisotropy is extended to the overall film instead of the step edge local effect. We speculate that anomalous behavior is caused by the strain built in the films since the lattice mismatch between Fe and Pt is substantial. We notice that the slope of H_c with thickness increases as α increases. This is because the T_c value is enhanced by the introduction of the step surface. For a fixed Fe thickness, the results at the larger vicinal angle involve a significant enhancement of T_c. The temperature at which measurement were made is thus further below T_c, since $T_c(\alpha)$ is enhanced with α. This results in the observed higher H_c values for the stepped surfaces.

To better understand the dependence of magnetic anisotropy upon the step density, we also performed polar SMOKE measurements as a function of α at different Fe thickness. The hysteresis loops for 1.6 and 2.2 ML Fe are plotted in Fig. 4 and the data for M_s and H_c are summarized in Fig. 5. The reason that the polar magnetization of the 2.2 ML Fe film is smaller than that of 1.6 ML is due to the spin reorientation from in plane to out of plane around 1.6 ML. It is clear that, as α increases, the magnetization increases. Our qualitative discussion above relates this to the polarization of Pt atoms at the step edges. For a high-vicinal-angle surface, the density of step edge atoms increases, as does the contribution from proximal Pt atoms, so the magnetization increases. The polarization of Pt atoms is expected to produce a linear dependence with α. However, the solid-line data fitting shown in Fig. 5(a) indicates that the magnetization increases quadratically on α. This discrepancy implies that there is an additional contribution to the magnetization in our system. We know that the magnetization scales with temperature further below T_c. The data in Fig. 5 confirm the fact that in the Fe/Pt system the step-induced anisotropy enhances T_c. At higher-vicinal-angle surfaces, the T_c value increases, and the magnetization at room temperature increases as it is further below T_c.

The H_c value increases with increasing α in all films, consistent with simulation[33] and theoretical calculations.[34] This behavior is consistent with the physical intuition that steps on a vicinal surface introduce pinning sites that impede the motion of domain walls. It was shown that the magnetic anisotropy in Fe films grown on stepped Ag(001) increases quadratically with increasing step density,[23,24] while the coercivity of Co/Cu(001) films increases almost linearly with

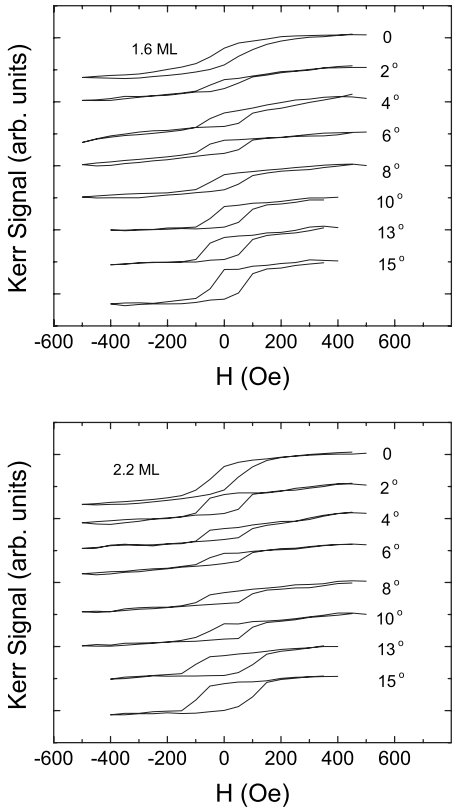

FIG. 4. Polar Kerr hysteresis loops at room temperature as a function of vicinal angle of Fe films grown on curved Pt(111) surface with indicated Fe thickness. (The coordinate axis scale is the same for the two figures.)

increasing step density.[26] Compared with the flat surface, the stepped surface introduces additional anisotropy. Shown as Fig. 5(b), H_c of thick Fe films shows a stronger dependence on α compared with low Fe coverage. This is related to the strain built into the film. The step-induced anisotropy extends over the entire film surface instead of being a local effect at the step edge.

Although the out-of-plane anisotropy of Fe on curved Pt(111) might result in antiferromagnetic ordering of adjacent steps due to dipolar interactions,[35,36] no sign of this was observed. We attribute this to the strong ferromagnetic polarization of the Pt substrate. Consider that when the spin reorientation transition occurs, the perpendicular anisotropy field compensates the in-plane demagnetizing field,[37] $2K_s(T,\alpha)/M_s d_{SR}=4\pi D_{eff} M_s$, where d_{SR} is the Fe coverage at the spin reorientation transition and D_{eff} is the effective demagnetization factor. First, we notice that d_{SR} is almost independent of T in our system;[29] this implies that the perpendicular surface anisotropy K_s has a T dependence that varies as $K_s(T) \propto M_s^2(T)$ due to the anisotropic Fe-Fe exchange coupling via the polarized Pt atoms. Second, d_{SR} is independent of α as illustrated in Fig. 3(a). This implies that the perpendicular surface anisotropy $K_s(\alpha)$ varies as $K_s(\alpha) \propto M_s^2(\alpha)$. Although the strong surface anisotropy does not show a dependence on α explicitly, the surface anisotropy does increase as the vicinal angle increases and depends on α as $K_s(\alpha) \propto \alpha^4$, since $M_s(\alpha)$ increases quadratically with α as discussed ear-

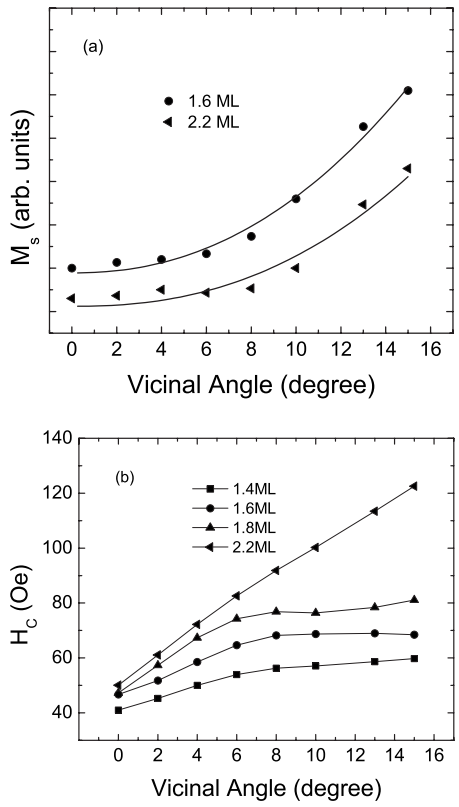

FIG. 5. (a) Magnetization M_s and (b) coercivity H_c of Fe grown on curved Pt(111) substrate as a function of vicinal angle at the indicated Fe thickness measured at room temperature via polar Kerr effect. [The solid lines in (a) are the fitted curves.]

lier. In our Fe/Pt system, the anisotropy shows a stronger dependence on α compared with other systems. In previous studies the step-induced anisotropy was found to depend linearly on the step density for Co/Cu,[26] and quadratically on step density for Fe/Ag.[23,24] The reason for the stronger dependence in our system is due to the contribution from both the step structure of the vicinal surface and the magnetic polarization of the Pt substrate. The step structure is related to the rotational symmetry breaking, and is also present in other systems, such as Fe/Ag and Co/Cu. However, magnetic polarization of the substrate does not exist in those systems; it is unique in our Fe/Pt system. Summarizing, the anisotropy of our Fe/Pt(111) system strongly depends on the vicinal angle and step density due to the contribution of symmetry-breaking-induced magnetic anisotropy and the proximal polarization of Pt atoms.

CONCLUSIONS

We investigated the growth and magnetic properties of ultrathin magnetic films of Fe grown on a curved Pt(111) vicinal single-crystal surface at room temperature. Pt is known to be nearly ferromagnetic and can have an induced magnetic moment when in proximity to 3*d* ferromagnetic atoms. The strong spin-orbit interaction in Pt produces a high value of the perpendicular magnetic anisotropy in the Fe/Pt system. We find that the step-induced magnetic anisotropy enhances the Curie temperature of the Fe ultrathin films. Both the saturated magnetization M_s and coercivity H_c of Fe grown on high-vicinal-angle surfaces show larger values compared with the flat surface. $M_s(\alpha)$ increases quadratically with α. The atomic steps of the vicinal surface greatly affect the magnetic properties of the ultrathin Fe films. Finally, we found that the step-induced surface anisotropy depends on α as $K_s(\alpha) \propto \alpha^4$. The reason for the stronger dependence in the Fe/stepped Pt(111) system is due to the contribution from both the step structure of the vicinal surface and the magnetic polarization of the Pt substrate.

ACKNOWLEDGMENT

Work at Argonne was supported by the U.S. Department of Energy, Office of Science, operating under Contract No. DE-AC02-06CH11357.

[1] F. J. Himpsel, J. E. Ortega, G. J. Mankey, and R. F. Willis, Adv. Phys. **47**, 511 (1998).
[2] C. Boeglin, S. Stanescu, J. P. Deville, P. Ohresser, and N. B. Brookes, Phys. Rev. B **66**, 014439 (2002).
[3] S. Rusponi, T. Cren, N. Weiss, M. Epple, P. Buluschek, L. Claude, and H. Brune, Nat. Mater. **2**, 546 (2003).
[4] F. Bisio, R. Moroni, F. Buatier de Mongeot, M. Canepa, and L. Mattera, Phys. Rev. Lett. **96**, 057204 (2006).
[5] H. J. Choi, Z. Q. Qiu, J. Pearson, J. S. Jiang, D. Q. Li, and S. D. Bader, Phys. Rev. B **57**, R12713 (1998).
[6] M. Komelj, D. Steiauf, and M. Fähnle, Phys. Rev. B **73**, 134428 (2006).
[7] J. M. Yeomans, *Statistical Mechanics of Phase Transitions* (Clarendon Press, Oxford, 1992), Chap. 5.
[8] N. D. Mermin and H. Wagner, Phys. Rev. Lett. **17**, 1133 (1966).
[9] M. Bander and D. L. Mills, Phys. Rev. B **38**, 12015 (1988).
[10] H. J. Elmers, J. Hauschild, H. Höche, U. Gradmann, H. Bethge, D. Heuer, and U. Köhler, Phys. Rev. Lett. **73**, 898 (1994).
[11] J. Shen, R. Skomski, M. Klaua, H. Jenniches, S. S. Manoharan, and J. Kirschner, Phys. Rev. B **56**, 2340 (1997).
[12] M. Pratzer, H. J. Elmers, M. Bode, O. Pietzsch, A. Kubetzka, and R. Wiesendanger, Phys. Rev. Lett. **87**, 127201 (2001).
[13] A. B. Shick, F. Máca, and P. M. Oppeneer, Phys. Rev. B **69**, 212410 (2004).
[14] P. Gambardella, A. Dallmeyer, K. Maiti, M. C. Malagoli, S. Rusponi, P. Ohresser, W. Eberhardt, C. Carbone, and K. Kern, Phys. Rev. Lett. **93**, 077203 (2004).
[15] B. Újfalussy, B. Lazarovits, L. Szunyogh, G. M. Stocks, and P. Weinberger, Phys. Rev. B **70**, 100404(R) (2004).
[16] D. Repetto, T. Y. Lee, S. Rusponi, J. Honolka, K. Kuhnke, V. Sessi, U. Starke, H. Brune, P. Gambardella, C. Carbone, A. Enders, and K. Kern, Phys. Rev. B **74**, 054408 (2006).
[17] K. Kuhnke and K. Kern, J. Phys.: Condens. Matter **15**, S3311 (2003).

[18] R. Robles, J. Izquierdo, and A. Vega, Phys. Rev. B **61**, 6848 (2000).
[19] J. Dorantes-Dávila and G. M. Pastor, Phys. Rev. Lett. **81**, 208 (1998); J. Dorantes-Dávila, H. Dreyssé, and G. M. Pastor, *ibid.* **91**, 197206 (2003).
[20] R. Félix-Medina, J. Dorantes-Dávila and G. M. Pastor, New J. Phys. **4**, 1001 (2002).
[21] J. Hong and R. Q. Wu, Phys. Rev. B **67**, 020406(R) (2003).
[22] H. J. Choi, R. K. Kawakami, E. J. Escorcia-Aparicio, Z. Q. Qiu, J. Pearson, J. S. Jiang, Dongqi Li, and S. D. Bader, Phys. Rev. Lett. **82**, 1947 (1999).
[23] R. K. Kawakami, E. J. Escorcia-Aparicio, and Z. Q. Qiu, Phys. Rev. Lett. **77**, 2570 (1996).
[24] Y. Z. Wu, C. Won, and Z. Q. Qiu, Phys. Rev. B **65**, 184419 (2002).
[25] L. Néel, C. R. Hebd. Seances Acad. Sci. **237**, 1468 (1953).
[26] Y. Z. Wu, C. Won, H. W. Zhao, and Z. Q. Qiu, Phys. Rev. B **67**, 094409 (2003).
[27] D. Weller, Y. Wu, J. Stöhr, M. G. Samant, B. D. Hermsmeier, and C. Chappert, Phys. Rev. B **49**, 12888 (1994).
[28] S. Papadia, M. C. Desjonqueres, and D. Spanjaard, Phys. Rev. B **53**, 4083 (1996).
[29] Ruihua Cheng, K. Yu. Guslienko, F. Y. Fradin, J. E. Pearson, H. F. Ding, Dongqi Li, and S. D. Bader, Phys. Rev. B **72**, 014409 (2005).
[30] Ruihua Cheng, J. Pearson, D. Li, and F. Y. Fradin, J. Appl. Phys. **100**, 073911 (2006).
[31] A. Berger, U. Linke, and H. P. Oepen, Phys. Rev. Lett. **68**, 839 (1992).
[32] D. Li, B. R. Cuenya, J. Pearson, S. D. Bader, and W. Keune, Phys. Rev. B **64**, 144410 (2001).
[33] D. Zhao, F. Liu, and D. L. Huber, J. Appl. Phys. **91**, 3150 (2002).
[34] R. A. Hyman, A. Zangwill, and M. D. Stiles, Phys. Rev. B **58**, 9276 (1998).
[35] J. Hauschild, H. J. Elmers, and U. Gradmann, Phys. Rev. B **57**, R677 (1998).
[36] Ya B. Losovyj, I. N. Yakovkin, H. K. Jeong, David Wisbey, and P. A. Dowben, J. Phys.: Condens. Matter **16**, 4711 (2004).
[37] B. Heinrich, J. F. Cochran, A. S. Arrott, S. T. Purcell, K. B. Urquhart, J. R. Dutcher, and W. F. Egelhoff, Appl. Phys. A: Solids Surf. **49**, 473 (1989).